C.P. No. 914

C.P. No. 914

MINISTRY OF AVIATION

AERONAUTICAL RESEARCH COUNCIL

CURRENT PAPERS

Measurement of the Internal Drag of Air Breathing Installations on Slender Wing-Body Combinations at Supersonic Speeds

by

J. W. Britton

LONDON: HER MAJESTY'S STATIONERY OFFICE

1967

FIVE SHILLINGS NET

U.D.C. No. 533.697 : 533.6.013.12 : 533.695.9 : 533.695.12 : 533.6.011.5

C.P. No.914*

December 1965

MEASUREMENT OF THE INTERNAL DRAG OF AIR BREATHING INSTALLATIONS ON SLENDER WING-BODY COMBINATIONS AT SUPERSONIC SPEEDS

by

J. W. Britton

SUMMARY

The problem of defining and measuring internal drag or thrust of a ducted body is discussed, and convenient methods of measurement are proposed. The accuracy of the internal drag measurement is considered, and the possibility of improving this accuracy by means of duct design is illustrated.

An account is given of the experimental techniques for measuring the internal and external drags of ducted models which are used in the 8 ft × 8 ft wind tunnel at R.A.E. Bedford.

---

*Replaces R.A.E. Tech. Report 65275 - A.R.C.27871

2

CONTENTS

1 INTRODUCTION

One of the problems arising in wind tunnel tests on models of specific aircraft or missiles is the treatment of the flow through and around the propulsion units. In general, it is necessary to represent correctly both the internal flow* ahead of the inlet (pre-entry flow) and the internal flow downstream of the exit (post-exit flow) in order to determine both the external flow effects and also the momentum change of the air accepted by the duct. The flow ahead of the intake can usually be represented on the model in the wind tunnel, although any difference between full scale and model scale Reynolds number can introduce a choice between an accurate scale model of the intake, and a modified form with the boundary layer removal devices (e.g. diverters) resized such that the correct relationship with the local boundary layer thickness is reproduced. Representation of the post-exit flow can be a particularly difficult problem, since a hot, high pressure jet must be simulated; but fortunately in many cases the location of the exit is such that this flow can have little influence on the forces acting on the external surfaces of the model and generally no attempt is made at accurate simulation.

This Report considers the problem of measuring the forces on a ducted model (and in particular the internal drag) when the pre-entry flow is adequately represented, and when it can be assumed that the post exit flow does not affect the external forces on the configuration. The internal drag is defined in the manner of Ref.1 as the sum of the pre-entry and intrinsic drags, and must be obtained from a measurement of the change in the properties of the internal flow between free-stream and the exit of the duct. The possibility of improving the accuracy of the measured internal drag by designing the duct for a particular exit Mach number is examined and illustrated by a simple example.

Results are given for a 1/30th scale model of an early version of the B...C./Sud "Concord" tested in the R...E. Bedford 8 ft x 8 ft tunnel at M = 2.2. On a configuration such as "Concord", the nacelles can be easily separated from the rest of the configuration, and the change in the overall forces due to the addition of the nacelles to the basic configuration can be measured. The drag penalty, in particular, can be quoted as an "installation drag", a definition of this quantity is suggested and measured values quoted**.

---

*Internal flow is the flow of fluid which passes through the duct, from free-stream far ahead to a station far behind the model.

**In the case of "Concord", for which the experimental technique described in this Report was developed, the geometry is such that flow leaving the nacelle could have some effect on the rear part of the fin and tail cone even at a Mach number of 2.2; however no allowances have been made for this effect in this Report.

2 FORCES ACTING ON THE COMPLETE CONFIGURATION

A discussion on the definition of the internal and external drags of a ducted body is given in Ref.1.

For the present investigation, internal drag is the sum of the longitudinal forces acting on the free boundaries of the pre-entry stream tube (i.e. pre-entry drag) and the surfaces of the body, up to the exit survey-plane, which are wetted by the internal flow (i.e. intrinsic drag). This definition of internal drag is very similar to the standard internal drag as defined in Ref.1. (The differences arise because the exit survey plane is just upstream of the duct exit, thus avoiding the difficulties associated with distinguishing between the internal, base and external flows in the exit plane itself; the internal drag due to that part of the duct between the exit flow survey plane and the duct exit is neglected.) Any drag due to the internal flow downstream of the duct exit plane is neglected.

The external drag is the sum of the longitudinal forces acting on the free boundaries of the pre-entry stream tube and those parts of the body which are wetted by the external flow but excluding any base area on the nacelles. Thus measured results have to be corrected for any base drag of the nacelles on the tunnel configuration.

Thus the full scale aircraft drag coefficient is:-

$$C_{D_{a/c}} = \left(C_{D_2} - C_{D_{base}} - C_{D_{internal}} - C_{D_{2f_{ext}}}\right)_{model} + \left(C_{D_{f_{ext}}}\right)_{a/c} \qquad (1)$$

where C_{D_2} is the drag coefficient measured at a given lift coefficient

and $C_{D_{2f_{ext}}}$ is the skin friction drag of that area of the complete configuration which is wetted by the external flow.

This aircraft external drag is associated with a thrust of the installed engine which is defined as the change of momentum and pressure forces from free-stream to nozzle exit of the engine flow. Corrections have to be made for the disposal of the boundary layer ahead (or underneath) the intake, e.g. a diverter drag, and the skin friction of the wing wetted by the pre-entry flow, and for any base drag or losses due to incorrect expansion of the jet.

It is often advantageous to be able to assess the penalties due to adding the nacelles to the basic wing/body combination. In this case we define an installation drag as the difference between the external pressure drag of the

complete configuration (excluding base drag) and the pressure drag of the configuration without nacelles at the same lift. If C_{D_1} is the wind tunnel measurement of the drag coefficient of the model without nacelles and C_{D_2} is the drag coefficient at the same lift of the model with nacelles and if the suffices "f" and "p" are used to identify the friction and pressure contributions respectively, then the installation drag coefficient $C_{D_{inst}}$ can be written as

$$C_{D_{inst}} = \left(C_{D_{2_{ext}}} - C_{D_{2_{ext_f}}}\right) - C_{D_{1p}} \tag{2}$$

where

$$C_{D_{2_{ext}}} = \left(C_{D_2} - C_{D_{base}}\right) - C_{D_{internal}} \tag{2a}$$

and

$$C_{D_{1p}} = C_{D_1} - C_{D_{1f}} \tag{2b}$$

then

$$C_{D_{inst}} = \left(C_{D_2} - C_{D_1}\right) - C_{D_{internal}} - C_{D_{base}} - \left(C_{D_{2_{ext_f}}} - C_{D_{1f}}\right). \tag{3}$$

Equation (1) can then be written in the alternative form

$$C_{D_{a/c}} = \left[C_{D_{1p}} + C_{D_{inst}}\right]_{model} + \left(C_{D_{f_{ext\ \ full\ scale}}}\right). \tag{4}$$

3 INTERNAL DRAG

In terms of the momentum and pressure of the internal flow at the relevant flow stations, the internal drag ($-\Theta_{sn}$) can be written as

$$-\Theta_{sn} = m_e V_\infty - \int_{A_e} \left(p_e - p_\infty + \rho_e V_e^2 \cos^2 \phi_e\right) dA \tag{6}$$

where

$$m_e = \int_{A_e} \rho_e V_e \, dA \tag{7}$$

for small values of ϕ_e, equation (6) reduces to

$$-\Theta_{sn} = m_e V_\infty - \int_{A_e} \left(p_e - p_\infty + \rho_e V_e^2 \right) dA \ . \tag{8}$$

If it is assumed that the stagnation temperature T_t is constant, equation (8) can be recast into the form (see Appendix A)

$$-\Theta_{sn} = \int_{A_e} p_e f_1(M_e) \, dA + p_\infty A_e \tag{9}$$

where

$$f_1(M_e) = \left\{ \gamma M_e^2 \left[\frac{V_\infty / a_*}{V_e / a_*} \right] - (1 + \gamma M_e^2) \right\} \ . \tag{10}$$

The problem of accurate evaluation of internal drag by means of the original equations (6) and (7) is aggravated by the requirement of two independent integrations of the relevant exit flow properties, and also by the fact that the difference between these integrations is usually an order of magnitude less than the integrations themselves. This problem is considerably reduced by using equations (9) and (10), since the need for two separate integrations is removed. Physically, equation (9) is the integration of the internal drag of each individual stream tube of the internal flow.

The variation of the function $f_1(M_e)$ with exit Mach number, which is shown in Fig.2, offers a further reduction of the problem of internal drag measurement. This effect is illustrated in Fig.3, where the error in measured internal drag caused by an error in either measured exit static or exit pitot pressure is shown for a range of free-stream and exit Mach numbers. For this example, a considerably simplified exit flow was considered where the properties of the internal flow and errors in measurement of these properties do not vary in the exit flow survey plane. Strictly the information in Fig.3 applies to the case where the internal

flow pressure recovery at exit is unity; however, changes in the pressure recovery produce only small variations from the data presented. It is clear from Fig.3(a) that the duct should be designed to have an exit Mach number of unity to minimise the effect of error in static pressure measurement for any free-stream Mach number. Fig.3(b), on the other hand, shows that the desired exit Mach number varies with free-stream Mach number if the effect of errors in pitot pressure measurement are to be minimised. Thus excepting the case of $M_\infty = 2.2$ when the desired exit Mach number from both considerations is unity, some compromise is involved in choosing the "best" exit Mach number.

Another interesting property of the function $f_1(M_e)$ is that for a free-stream Mach number of 2.2, and a duct exit Mach number of 1.0, $f_1(M_e)$ is very small; so that for a perfect sonic duct exit the internal drag (equation (9)) depends only on the physical size of the exit and the conditions in free-stream, both of which are readily available.

4 EXPERIMENTAL TECHNIQUES

4.1 The flow inside the duct

Two different types of ducts have been used in tests on a 1/30th scale model of a complete configuration of the B.A.C./Sud "Concord" in the 8 ft x 8 ft wind tunnel at R.A.E. Bedford. The first type had simple internal geometry - the cross-sectional area of the duct was constant, and changes of duct section shape were minimised. For the second type, a more sophisticated internal geometry was designed, to produce the desired duct exit Mach number - as defined in section 3. The inlets of both ducts were simplified and inlet compression ramps and boundary layer diverters, bleeds etc. were omitted. Thus the duct inlet flow, which included the boundary layer of that part of the model wetted by the pre-entry flow, did not pass through the intake shock geometry.

4.1.1 The constant cross-sectional area duct

The characteristics of this type of duct are very similar to those of the straight parallel ducts with pitot inlets which are considered in Ref.2. The boundary layer growth inside the duct effectively makes the duct convergent; so that for inlet Mach numbers above a critical value, at which the duct is just choked by the boundary layer growth, the flow inside the duct is supersonic. For inlet Mach numbers below this critical value, a complicated inlet shock wave pattern, associated with flow spillage at the inlet is established.

4.1.2 The duct with choked exit

It was noted in section 3, from a consideration of the function $f_1(M_e)$, that for a free-stream Mach number, $M_\infty = 2.2$, the required exit Mach number was approximately unity. Thus a duct design is required such that sonic conditions are obtained in the exit flow, and also such that the pre-entry flow is unaffected by the flow inside the duct. A convergent-divergent-convergent duct will give these conditions; the flow inside such a duct is intended to go through the following stages (Fig.4)

(i) Supersonic isentropic compression to the first throat.

(ii) Supersonic expansion to the normal shock.

(iii) Subsonic diffusion to the beginning of the choking wedges.

(iv) Subsonic acceleration to the sonic throat.

Since in practice there is a boundary layer on the walls of the duct, (this boundary layer is particularly thick on the wing surface, which forms one of the duct walls) the classical single normal shock is replaced by a series of bifurcated normal shocks to form a "compression region". (This type of flow is considered in some detail in Refs.3 and 4.) The length of this compression region depends on the nature and thickness of the boundary layer with which it interacts, and also on the incident Mach number.

The minimum Mach number obtainable at the first throat is associated with the maximum contraction from inlet to first throat which will also allow the duct to start. Simple considerations of continuity and normal shock pressure recovery for the starting operation for a free-stream Mach number of $M_\infty = 2.8$ (maximum obtainable in 8 ft x 8 ft wind tunnel) indicate a maximum contraction ratio of 1.36, thus for an inlet Mach number $M_i \doteqdot 2.1$ the Mach number at the first throat is $M \doteqdot 1.7$. However, since the flow configuration during the starting operation is not precisely known, a throat Mach number of $M \doteqdot 1.8$ was selected as a practical minimum value.

The duct exit area is chosen such that the compression region in the diffuser is just downstream of the first throat. For this particular model, the duct-exit size was obtained from a pilot experiment; however, simple one dimensional analysis of the flow between the first throat and the exit can indicate an approximate value of this area. (Normal shock pressure recovery for the "compression region" can be assumed - see Refs. 3 and 4.)

The smooth shape of the duct floor between the inlet and the beginning of the choking wedges was designed so that severe adverse pressure gradients which

might have caused boundary layer separation in the contraction were avoided, and so that the total divergence angle of the diffuser was approximately 5° (Refs.3 and 4 indicate that this angle could be increased to 6° without penalty.). The profile of the choking wedges was divided into three sections; the initial straight line profile gave a total convergence angle of about 20°, this was followed by a circular arc profile (radius $\div$ 8 x local duct height) and finally a further straight line profile which gave a parallel duct about $\frac{3}{4}$ inch long in the free-stream direction with the model at the cruising attitude.

The required duct exit flow conditions can also be obtained using a special case of the "con-di-con" duct - this is the divergent-convergent duct. The flow inside this type of duct is intended to go through the last three stages only of the sequence suggested for the "con-di-con" duct, and since there is no initial internal contraction the "di-con" duct does not have the starting problems associated with the "con-di-con" duct. The diffuser of the "di-con" duct effectively begins at the duct inlet, but it is essential that a duct exit area is chosen such that the compression region is kept well downstream of the intake (at least 2h, where h is the distance from the inlet cowl lip to the local wing surface) so as to avoid any possible interference with the pre-entry flow.

For this particular model, the length of the duct is rather short (about 10h), and it was decided that the best solution to the problem of containing the compression region in the available diffuser length was offered by the "con-di-con" duct, which has the much shorter compression region associated with the lower incident Mach number and lower local duct "diameter" of this type of duct. For configurations with longer ducts than the present, the "di-con" duct may be the better type to choose.

4.1.3 Comparison of the constant area duct and the "con-di-con" duct

The main advantages of the constant area duct are the obvious simplicity of design and manufacture and the fact that satisfactory supercritical flow can be obtained for a wide range of inlet Mach numbers. This contrasts with the "con-di-con" duct which requires careful design for each inlet condition in order to obtain just supercritical flow in the duct, although small variations in inlet Mach number ($\Delta M \div 0.1$) can usually be accommodated without producing either sub-critical flow or over-supercritical flow - which aggravates further the problem of containing the compression region in the diffuser.

The main advantages of the "con-di-con" duct are (i) an exit Mach number can be obtained such that the susceptibility of the measured internal drag to errors in exit flow measurement (Fig.3) is minimised and (ii) the pressure

distributions in the exit flow are smooth. In contrast, the simpler duct usually produces an exit Mach number far from this "optimum" value, and this disadvantage is magnified by the fact that exit flow measurement is made more difficult by disturbances which might originate in the forward part of the duct due to non-uniform or misaligned inlet flow and are perpetuated to the flow measuring station at the exit. These effects are illustrated in Fig.5 where typical pressure and Mach number distributions across the centre line of the exit of each type of duct are shown.

Thus, when an accurate measurement of internal drag is of prime importance, the con-di-con duct is seen to be superior to the constant area duct; it has, however, the disadvantage of a much smaller range of inlet conditions for a fixed duct geometry.

4.2 Details of tests

Two comprehensive surveys of the nacelle exit flow were made using (i) a single static pressure probe and (ii) a four tube pitot pressure rake. The rakes were mounted on a remotely controlled traversing arm which is shown in Fig.1. The movement of traversing arm (i.e. primary, secondary and tertiary rotations, and fore and aft translation) was monitored so that the position of the arm in the exit flow was known; contact between the probe and the walls of the duct was indicated electrically. For a nacelle exit area of some three square inches, about 50 static pressure and about 120 pitot pressure measurements were made in the "con-di-con" duct; about 100 static pressures and about 200 pitot pressures were necessary in the more complicated exit flow of the constant area duct. The pressure traverses were made in a plane parallel to the duct exit plane and 0.25 inch upstream of the exit.

The pressures acting on the blunt base of the nacelle were measured using static pressure orifices in the base itself. The skin friction drag of the base was negligible.

The overall forces acting on the basic and complete configurations were measured with boundary layer transition artificially fixed near the leading edges of the wings, near the nose of the body, and near the leading edges of the nacelle cowl (for both internal and external flows) by means of a narrow band of distributed roughness*. The models were supported in the wind tunnel on a $2\frac{1}{4}$ inches diameter six component strain gauge balance and a 2.1 inches diameter rear sting.

---

*A full discussion of this technique is given in Ref.5.

The experimental work necessary for the determination of the installation drag falls into five parts:-

(i) Overall force test on the basic configuration.

(ii) Test on the complete configuration in which the pressures on the base of the nacelle and on the walls of the duct were measured.

(iii) Measurement of the static pressure distribution in the exit flow.

(iv) Measurement of the pitot pressure distribution in the exit flow.

(v) Overall force measurement of the complete configuration.

In the 8 ft x 8 ft wind tunnel at R.A.E. Bedford, this sequence can be completed in three "tunnel runs", with the last three parts being covered in a single "run". During the overall force measurement in the final run the traversing arm was retracted so that there was no possible interference from the probe on the flow over the model.

4.3 Skin friction

The skin friction drags of those parts of the model which are required in the evaluation of the installation drag were estimated using the curves of Ref.6 for the skin friction on a flat plate in zero pressure gradient.

5 THE NACELLE INSTALLATION DRAG OF "CONCORD"

The experimental and analytical techniques outlined in the preceding sections have been used in the analysis of the nacelle installation drag of the B.A.C./Sud "Concord" aircraft.

In this particular case it was assumed that the external skin friction drag of the complete configuration excluding nacelles (i.e. the area A in Fig.6) can be removed from each skin friction drag term in equation (4). These become:

(i) the skin friction drag of the nacelle surface wetted by the external flow,

(ii) the skin friction drag of those parts of the basic configuration, which are not wetted by the external flow on the complete configuration (i.e. the area B in Fig.6).

Thus the expression for the installation drag becomes

$$D_{inst} = (D_2 - D_1) - \text{internal drag} - \text{base drag} - \text{skin friction drag of nacelle surface wetted by external flow} + \text{skin friction drag of area B on basic configuration} \quad \ldots (11)$$

(For the rectangular box nacelle shape of the "Concord", a further simplification can be obtained since the skin friction drag of the nacelle lower surface is approximately equal to the skin friction drag of those parts of the basic configuration which are not wetted by pre-entry flow or external flow on the complete configuration (i.e. the area C in Fig.6).)

A specimen evaluation of the nacelle installation drag for one version of the "Concord" is presented in Table 1 - the drag components have been expressed in the usual coefficient form based on a reference wing area. The installation drags quoted are for the same external configuration, and whilst the difference between the values is small, slightly more confidence can be placed in that obtained from the configuration with the "con-di-con" duct because of the reduction in the errors which might arise from the internal drag in this case. The tabulated values also illustrate the relative sizes of the terms involved in the evaluation of the installation drag.

The internal drag of the constant area duct can be compared to the estimated internal skin friction drag - $C_{D_{f_{int}}} = 0.0016$. It was assumed here that the Mach number at the edge of the internal boundary layer was M = 2.0 throughout, and that there was no loss of total pressure in the supersonic core of the internal flow. The good agreement here is remarkable in view of the crude assumptions involved in obtaining the skin friction drag.

The internal drag of the "con-di-con" duct can be compared to that of a duct with a sonic exit. In these circumstances equation (9) reduces to:

$$- \theta_{sn} = \left[f_1(M_{1.0}) \right]_{M_\infty = 2.2} \int_{A_e} p_e \, dA + p_\infty A_e \quad . \tag{12}$$

This expression is equivalent to that obtained in Ref.7 (equation (6)) which was written as:

$$C_{D_{int}} = \frac{p_\infty}{q_\infty} \left(1 - \frac{P_e}{H_\infty} B_\infty \right) \frac{A_e}{S} \tag{13}$$

where

$$B_\infty = 1.268 \frac{H_\infty}{p_\infty} - \frac{2q_\infty}{p_\infty} \left(\frac{\dot{m}}{\dot{m}^*} \right)_\infty \tag{14}$$

and $\frac{P_e}{H_\infty}$ is the mean (area weighted) pressure recovery at the exit.

For this duct (with sonic exit) $C_{D_{int}} = 0.0036$ which is considerably greater than the measured value, due to the deviation from $M_e = 1.0$ in the exit flow.

The duct exit shape was intended to produce a choked exit with near sonic Mach numbers and a conventional sonic line shape and position. However, the upstream compression region produces very thick boundary layers in the diffuser and non-linear conditions in the "settling chamber" ahead of the contraction, which gives a flow which differs from that normally encountered at the geometric throat of a choked exit.

6 CONCLUDING REMARKS

The internal drag of a ducted configuration has been considered in some detail, and methods for designing the duct shape have been proposed so that the accuracy of an indirect measurement of this internal drag can be improved.

The experimental techniques used for measuring the internal and external drags of ducted models of a configuration of the B.A.C./Sud Concord aircraft in the 8 ft × 8 ft wind tunnel at R.A.E. Bedford have been described. Results from two methods of internal drag measurement have been compared.

Appendix A

FORMULAE FOR INTERNAL DRAG

In Ref.1 the internal drag of a ducted installation is given as:

$$\Theta_{sn} = m_i V_\infty - \int_{A_e} p_e - p_\infty + \rho_e V_e^2 \cos^2 \phi_e \, dA \qquad (A.1)$$

when ϕ_e is small, this expression can be approximated to:

$$-\Theta_{sn} = m_i V_\infty - \int_{A_e} p_e - p_\infty + \rho_e V_e^2 \, dA \; . \qquad (A.2)$$

Now

$$m_i = m_e = m_\infty = \int_{A_\infty} \rho_\infty V_\infty \, dA = \int_{A_e} \rho_e V_e \, dA \qquad (A.3)$$

therefore

$$-\Theta_{sn} = \int_{A_e} \rho_e V_e V_\infty \, dA - \int_{A_e} p_e - p_\infty + \rho_e V_e^2 \, dA \qquad (A.4)$$

$$= \int_{A_e} \gamma p_e M_e^2 \frac{V_\infty}{V_e} \, dA - \int_{A_e} p_e - p_\infty + \gamma p_e M_e^2 \, dA \qquad (A.5)$$

$$= \int_{A_e} p_e \left(\gamma M_e^2 \frac{V_\infty}{V_e} - 1 + \gamma M_e^2 \right) dA + p_\infty A_e \; . \qquad (A.6)$$

If we assume that the total temperature T_t is constant, then a_* is constant.

$$-\Theta_{sn} = \int_{A_e} p_e \left\{ \gamma M_e^2 \left[\frac{(V/a_*)_\infty}{(V/a_*)_e} \right] - (1 + \gamma M_e^2) \right\} dA + p_\infty A_e \qquad (A.7)$$

i.e.

$$-\Theta_{sn} = \int_{A_e} p_e f_1(M_e) \, dA + p_\infty A_e \qquad (A.8)$$

where

$$f_1(M_e) = \left\{ \gamma M_e^2 \left[\frac{(V/a_*)_\infty}{(V/a_*)_e} \right] - (1 + \gamma M_e^2) \right\} \; . \qquad (A.9)$$

Table 1

SPECIMEN NACELLE INSTALLATION DRAG EVALUATION

(Common external configuration)

$C_L = 0.1$ $M_\infty = 2.2$ Duct shape	$R = 2 \times 10^6$/ft Constant area duct	$R = 3 \times 10^6$/ft "Con-di-con" duct
$C_{D_{complete\ config.}} - C_{D_{basic\ config.}}$	0.00415	0.00560
Internal drag	0.00165	0.00316
	0.00250	0.00244
Base drag	0.00139	0.00130
	0.00111	0.00114
Skin friction drag of nacelle surface wetted by external flow	0.00097	0.00091
	0.00014	0.00023
Skin friction drag of area B on basic configuration	0.00062	0.00058
Installation drag	0.00076	0.00081

SYMBOLS

D	drag
D_1	drag of basic configuration
D_2	drag of complete configuration
D_{inst}	installation drag
p	static pressure
P	pitot pressure
H	total pressure
A	area
$-\Theta_{sn}$	internal drag
m	mass flow
V	velocity
ρ	density
ϕ	angle between local flow direction and free-stream
M	Mach number
R	Reynolds number
a_*	critical speed of sound
T_t	total temperature
C_D	drag coefficient $= \frac{D}{q_\infty S}$
C_L	lift coefficient $= \frac{L}{q_\infty S}$
q	dynamic pressure
S	wing reference area
h	distance from duct inlet cowl lip to local wing surface

Subscripts

∞	conditions in free-stream
i	conditions at duct inlet
e	conditions at internal flow measuring station 0.25 inch upstream of duct exit
1	refers to basic configuration
2	refers to complete configuration
p	as in D_p indicates pressure drag
f	as in D_f indicates skin friction drag
a/c	as in $D_{a/c}$ indicates aircraft drag
ext	refers to external flow
int	refers to internal flow

REFERENCES

No.	Author	Title, etc
1	-	*Report of the Definitions Panel on the definitions of the* thrust of a jet engine and of the internal drag of a ducted body. A.R.C. C.P.190, May 1954
2	J. Seddon	The flow through short straight pipes in a compressible viscous stream. A.R.C. C.P.355, April 1955
3	E.P. Neumann F. Lustwerk	Supersonic diffusers for wind tunnels. J. Appl. Mech. Vol.16, No.2, 1949
4	F. Lustwerk	The influence of the boundary layer on the "normal" shock configuration. M.I.T. Meteor Report No.61, 1950
5	J.Y.G. Evans	Use of a wind tunnel to determine the performance of slender wings suitable for a supersonic transport aircraft. A.R.C. C.P.824, August 1964
6	K.G. Smith	Methods and charts for estimating skin friction drag in wind tunnel tests with zero heat transfer. A.R.C.26469, 1964
7	L.E. Fraenkel	The external drag of some pitot-type intakes at supersonic speeds - Part 1. A.R.C.13537, June 1950

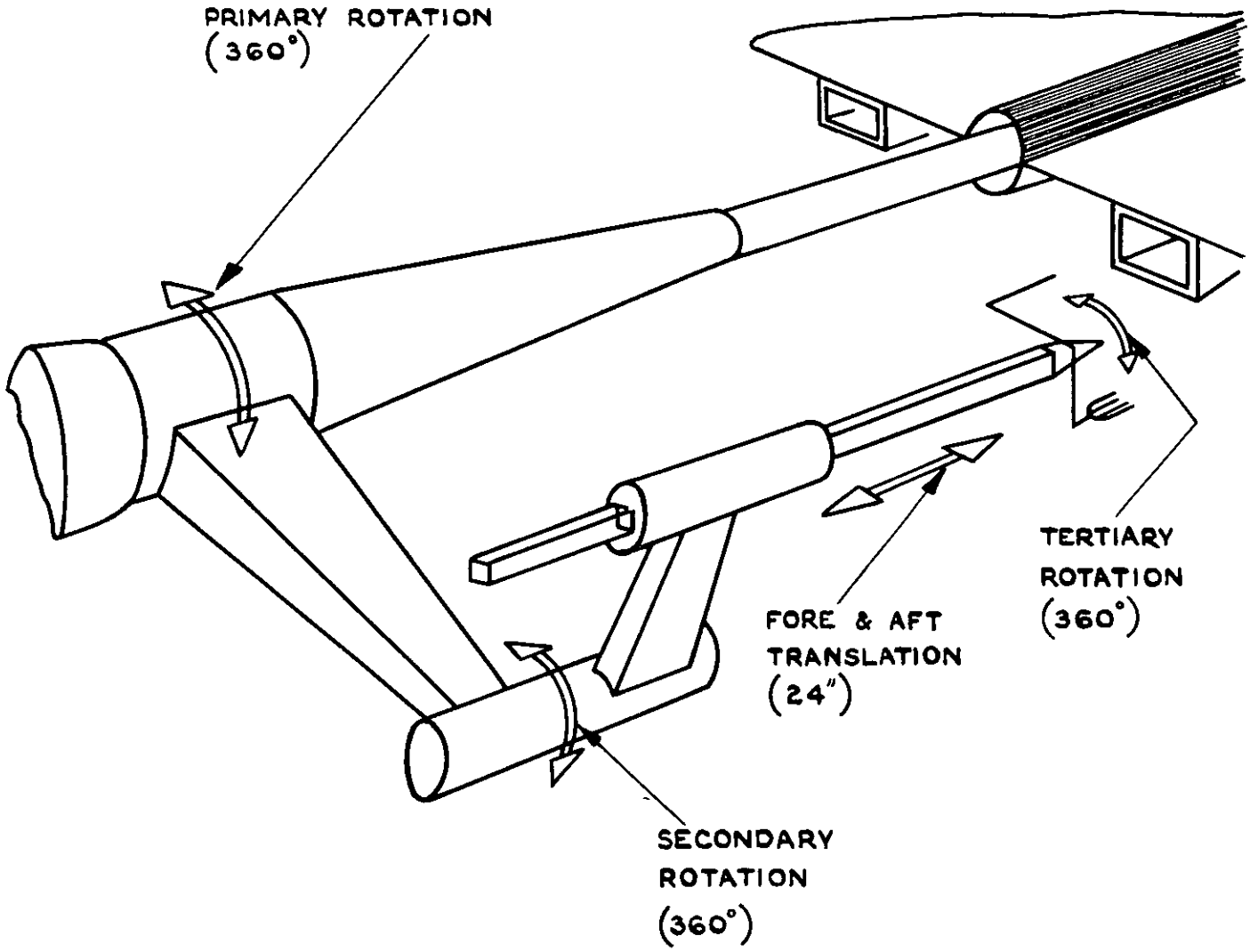

FIG. 1 DIAGRAM OF TRAVERSING ARM ARRANGEMENT USED IN DUCT EXIT FLOW SURVEYS

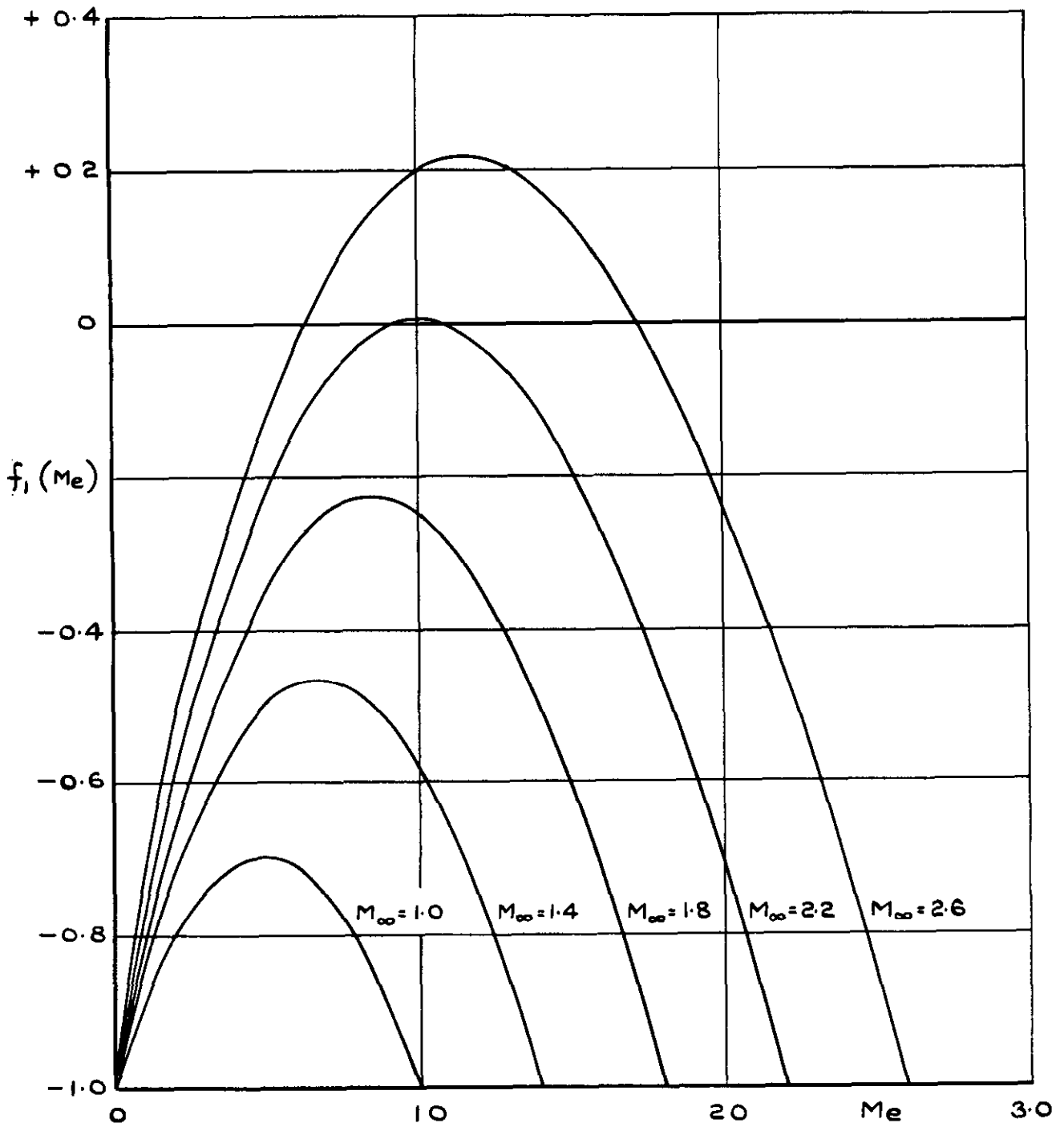

FIG. 2 VARIATION OF $f_1(M_e)$ WITH EXIT MACH NUMBER AND FREESTREAM MACH NUMBER

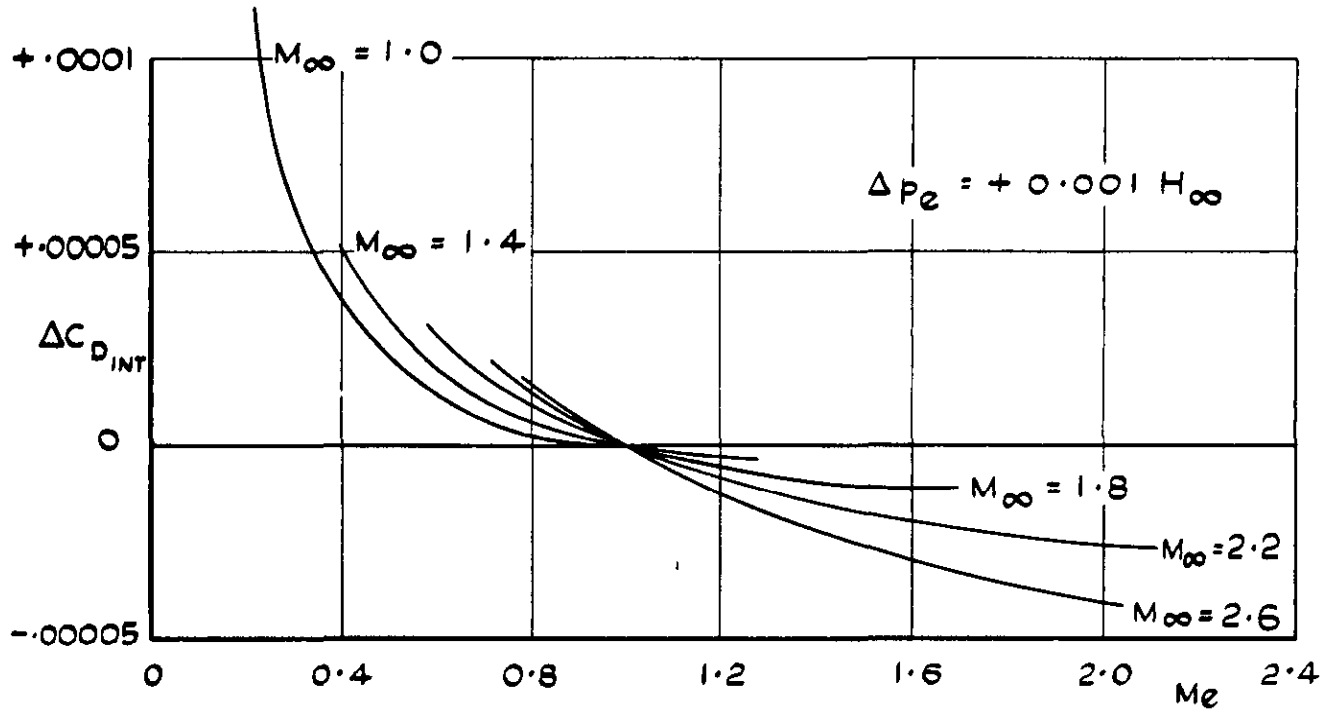

(a) EFFECT OF ERROR IN MEASURED EXIT STATIC PRESSURE.

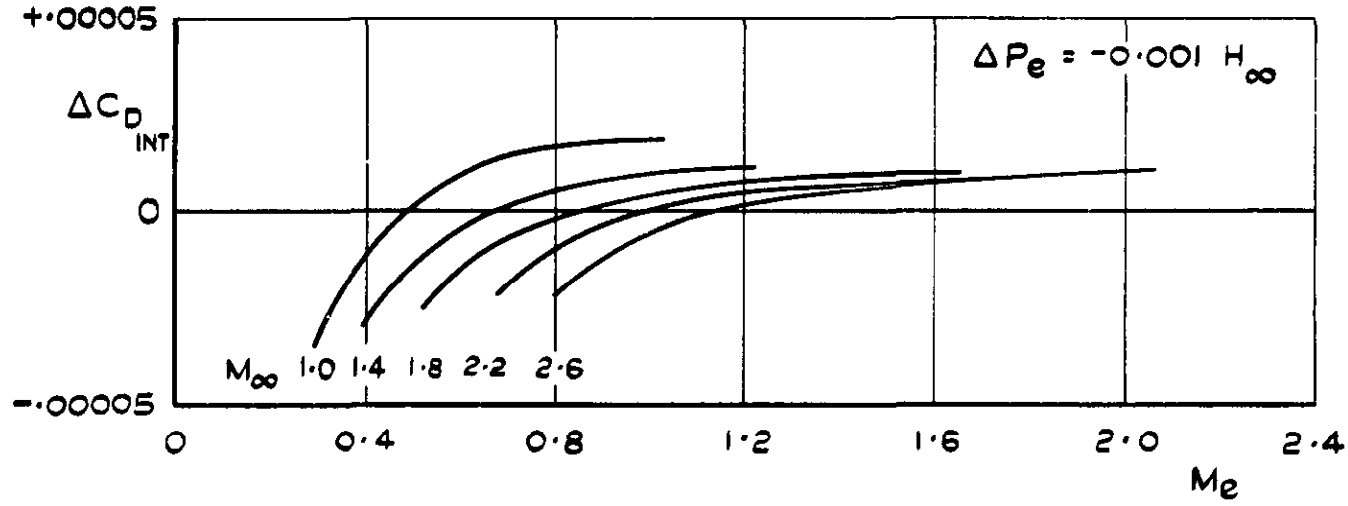

(b) EFFECT OF ERROR IN MEASURED EXIT PITOT PRESSURE.

FIG. 3 ERROR IN INTERNAL DRAG COEFFICIENT DUE TO ERROR IN PRESSURE MEASUREMENT AT DUCT EXIT

[DRAG COEFFICIENTS BASED ON REF AREA OF 500 SQ. INS.
DUCT EXIT AREA = 6 SQ INS]

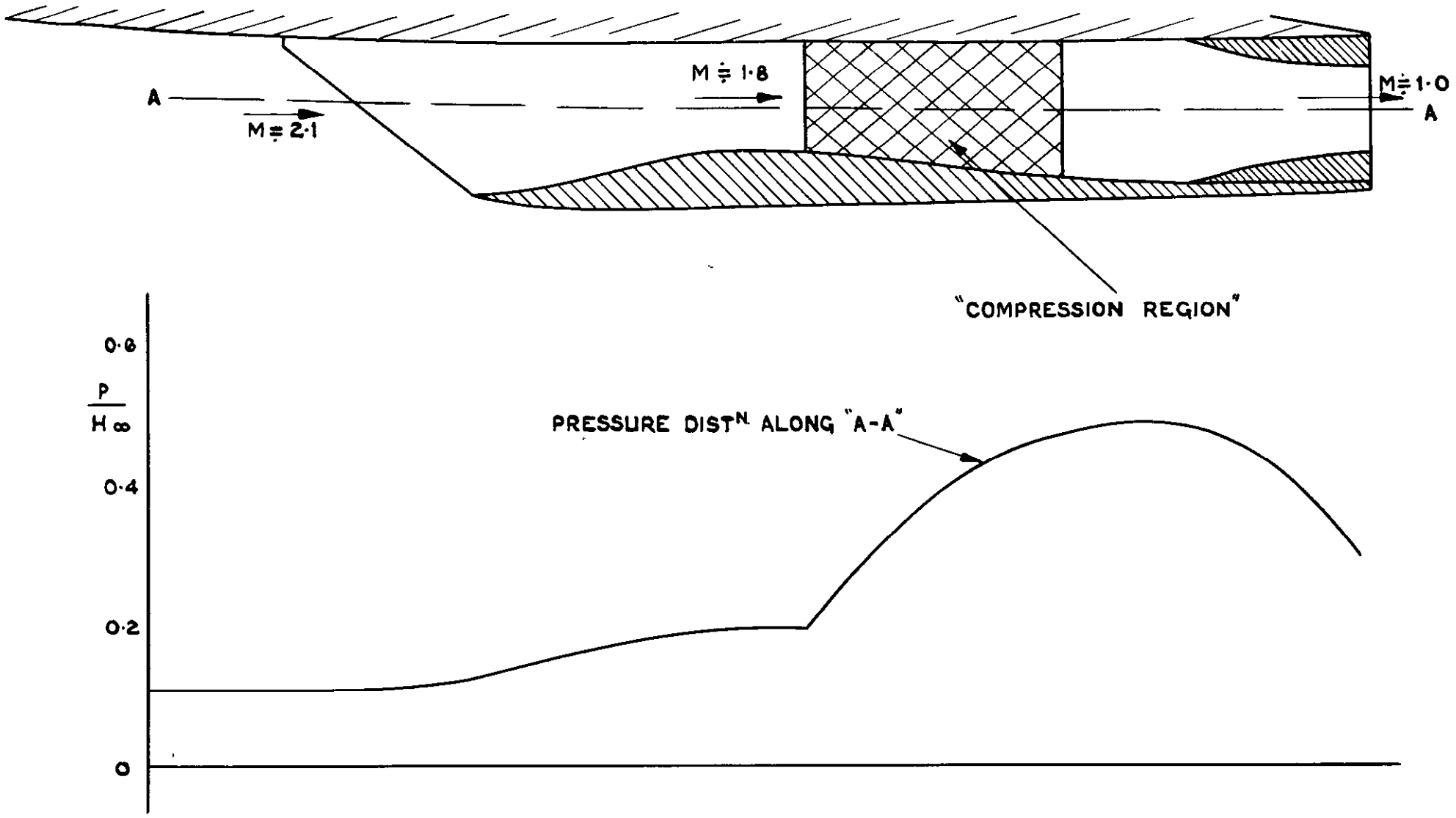

FIG. 4 DIAGRAM OF FLOW INSIDE CONVERGENT – DIVERGENT – CONVERGENT DUCT, AND A TYPICAL SIDE WALL PRESSURE DISTRIBUTION.

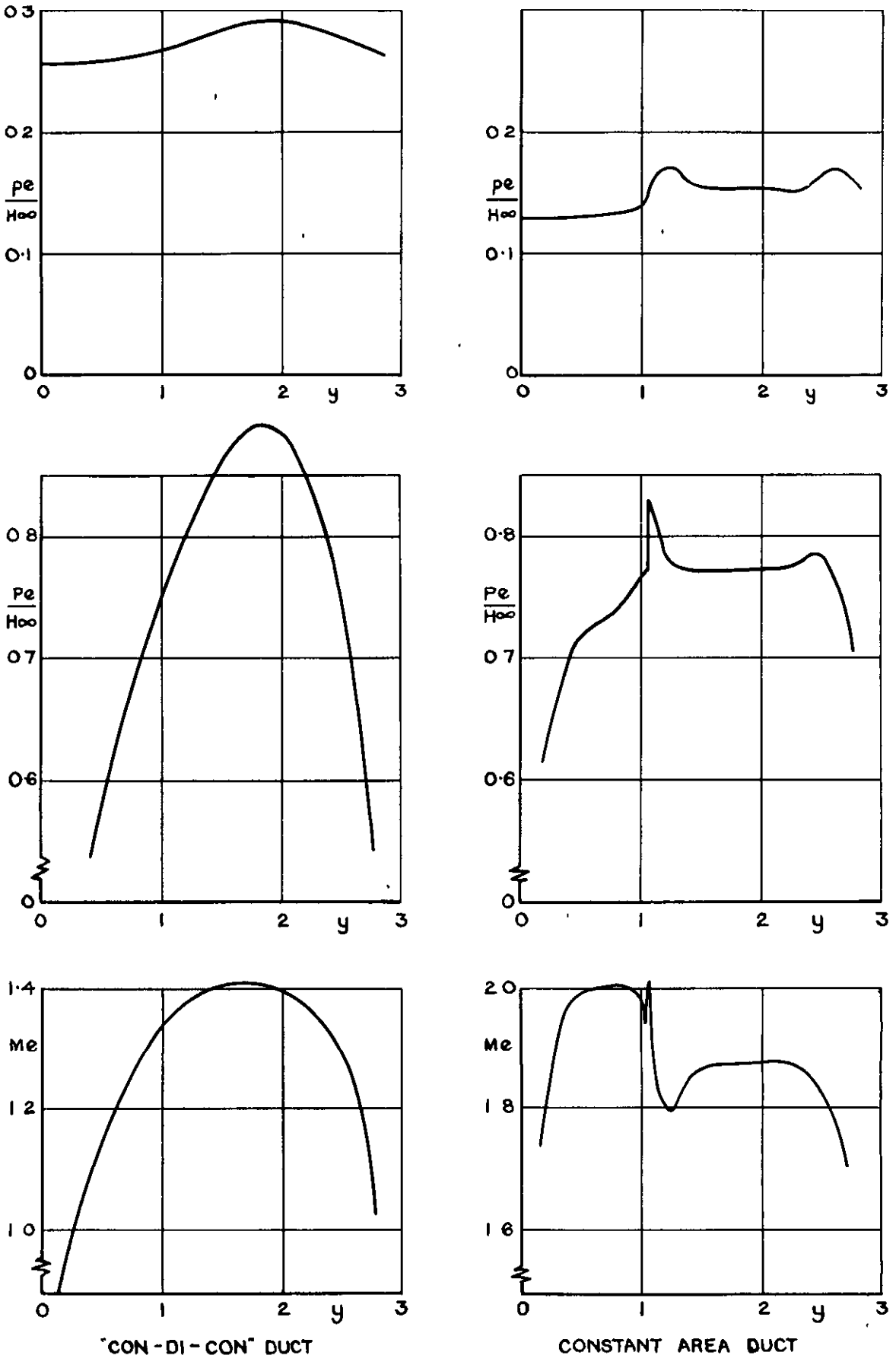

FIG. 5 TYPICAL PRESSURE AND MACH NUMBER DISTNS. ACROSS DUCT EXITS

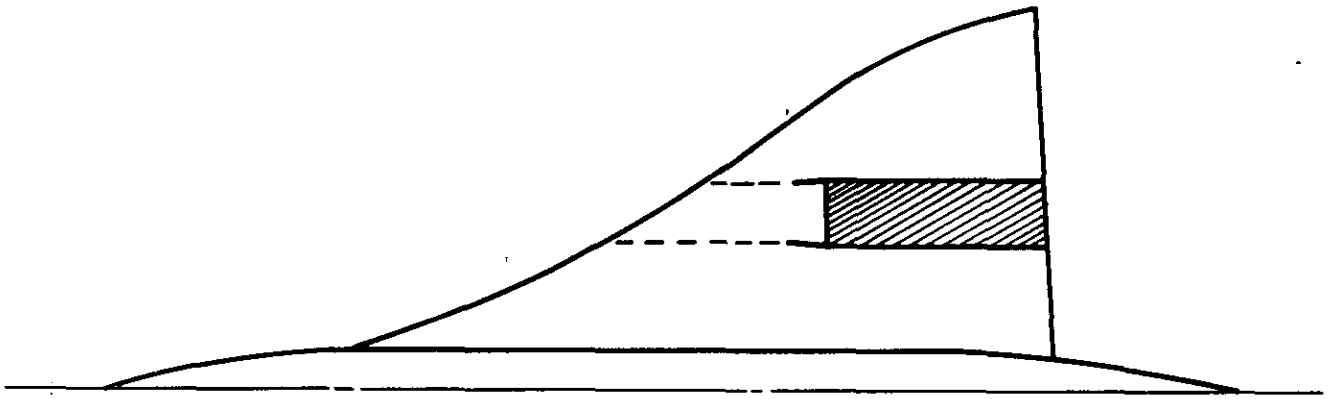

FIG 6a POSITION OF THE NACELLE ON THE WING LOWER SURFACE OF COMPLETE CONFIGURATION

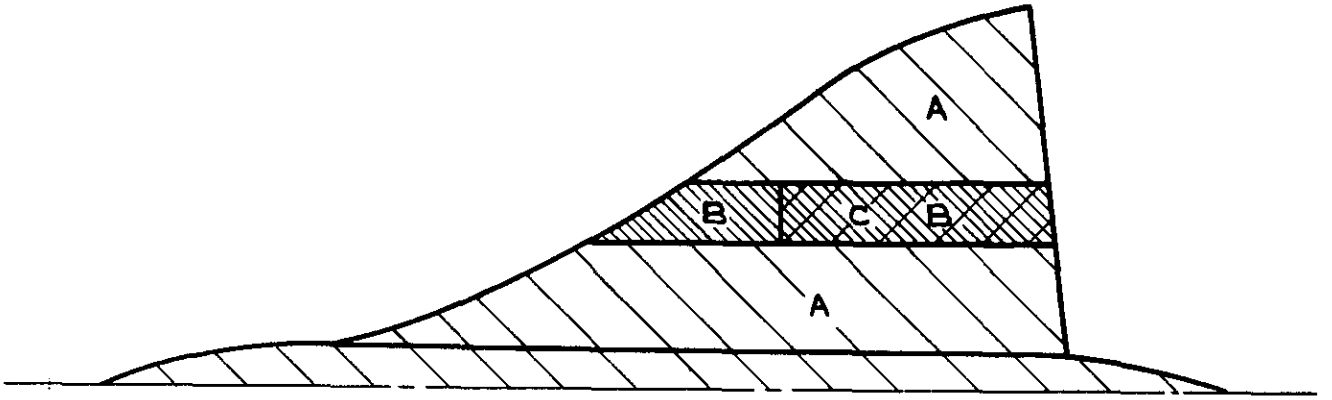

FIG 6 b REGIONS OF THE WING LOWER SURFACE OF THE BASIC CONFIGURATION AS DEFINED IN SECTION 5

Printed in England for Her Majesty's Stationery Office by the Royal Aircraft Establishment, Farnborough. Dd.125875.K.5.

A.R.C. C.P. No.914
December 1965
Britton, J. W.
MEASUREMENT OF THE INTERNAL DRAG OF AIR BREATHING INSTALLATIONS ON SLENDER WING-BODY COMBINATIONS AT SUPERSONIC SPEEDS

533.697 : 533.6.013.12 : 533.695.9 : 533.695.12 : 533.6.011.5

The problem of defining and measuring internal drag or thrust of a ducted body is discussed, and convenient methods of measurement are proposed. The accuracy of the internal drag measurement is considered, and the possibility of improving this accuracy by means of duct design is illustrated.

An account is given of the experimental techniques for measuring the internal and external drags of ducted models which are used in the 8 ft x 8 ft wind tunnel at R.A.E. Bedford.

A.R.C. C.P. No.914
December 1965
Britton, J.W.
MEASUREMENT OF THE INTERNAL DRAG OF AIR BREATHING INSTALLATIONS ON SLENDER WING-BODY COMBINATIONS AT SUPERSONIC SPEEDS

533.697 : 533.6.013.12 : 533.695.9 : 533.695.12 : 533.6.011.5

The problem of defining and measuring internal drag or thrust of a ducted body is discussed, and convenient methods of measurement are proposed. The accuracy of the internal drag measurement is considered, and the possibility of improving this accuracy by means of duct design is illustrated.

An account is given of the experimental techniques for measuring the internal and external drags of ducted models which are used in the 8 ft x 8 ft wind tunnel at R.A.E. Bedford.

A.R.C. C.P. No.914
December 1965
Britton, J. W.
I EASUREIENT OF THE INTERNAL DRAG OF AIR BREATHING INSTALLATIONS ON SLENDER WING-BODY COMBINATIONS AT SUPERSONIC SPEEDS

533.697 : 533.6.013.12 : 533.695.9 : 533.695.12 : 533.6.011.5

The problem of defining and measuring internal drag or thrust of a ducted body is discussed, and convenient methods of measurement are proposed. The accuracy of the internal drag measurement is considered, and the possibility of improving this accuracy by means of duct design is illustrated.

An account is given of the experimental techniques for measuring the internal and external drags of ducted models which are used in the 8 ft x 8 ft wind tunnel at R.A.E. Bedford.

DETACHABLE ABSTRACT CARDS

Published by
HER MAJESTY'S STATIONERY OFFICE

To be purchased from
49 High Holborn, London W C 1
423 Oxford Street, London W 1
13A Castle Street, Edinburgh 2
109 St Mary Street, Cardiff
Brazennose Street, Manchester 2
50 Fairfax Street, Bristol 1
35 Smallbrook, Ringway, Birmingham 5
80 Chichester Street, Belfast 1
or through any bookseller

S.O CODE No 23-9017-14